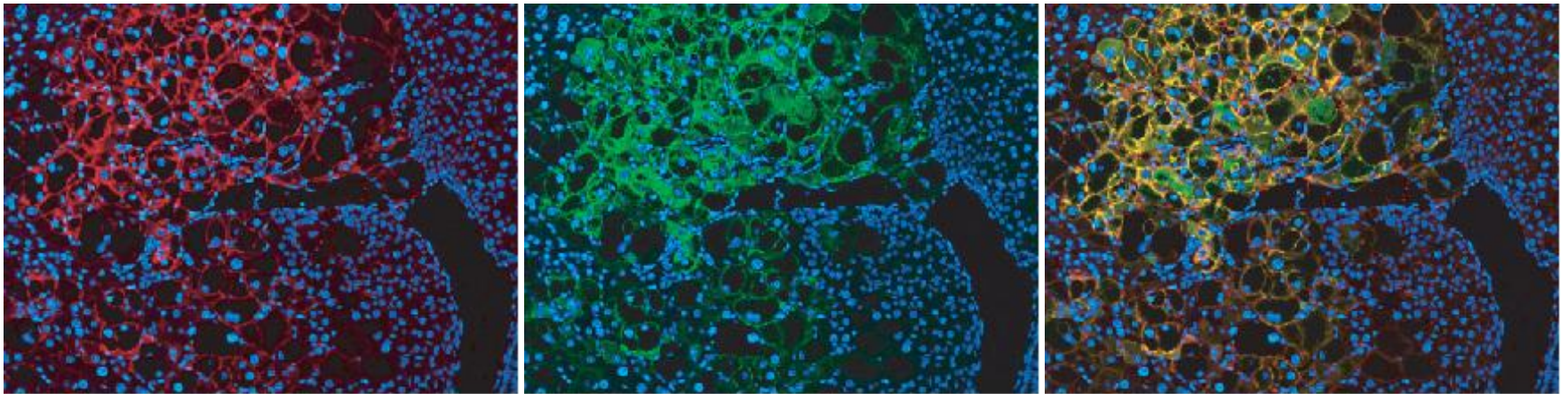


Supplementary Fig. 1. Macroscopic pictures of livers from wild-type (WT), AKT- and AKT/Spry2Y55F-injected mice 14 weeks post-injection (W.P.I.).

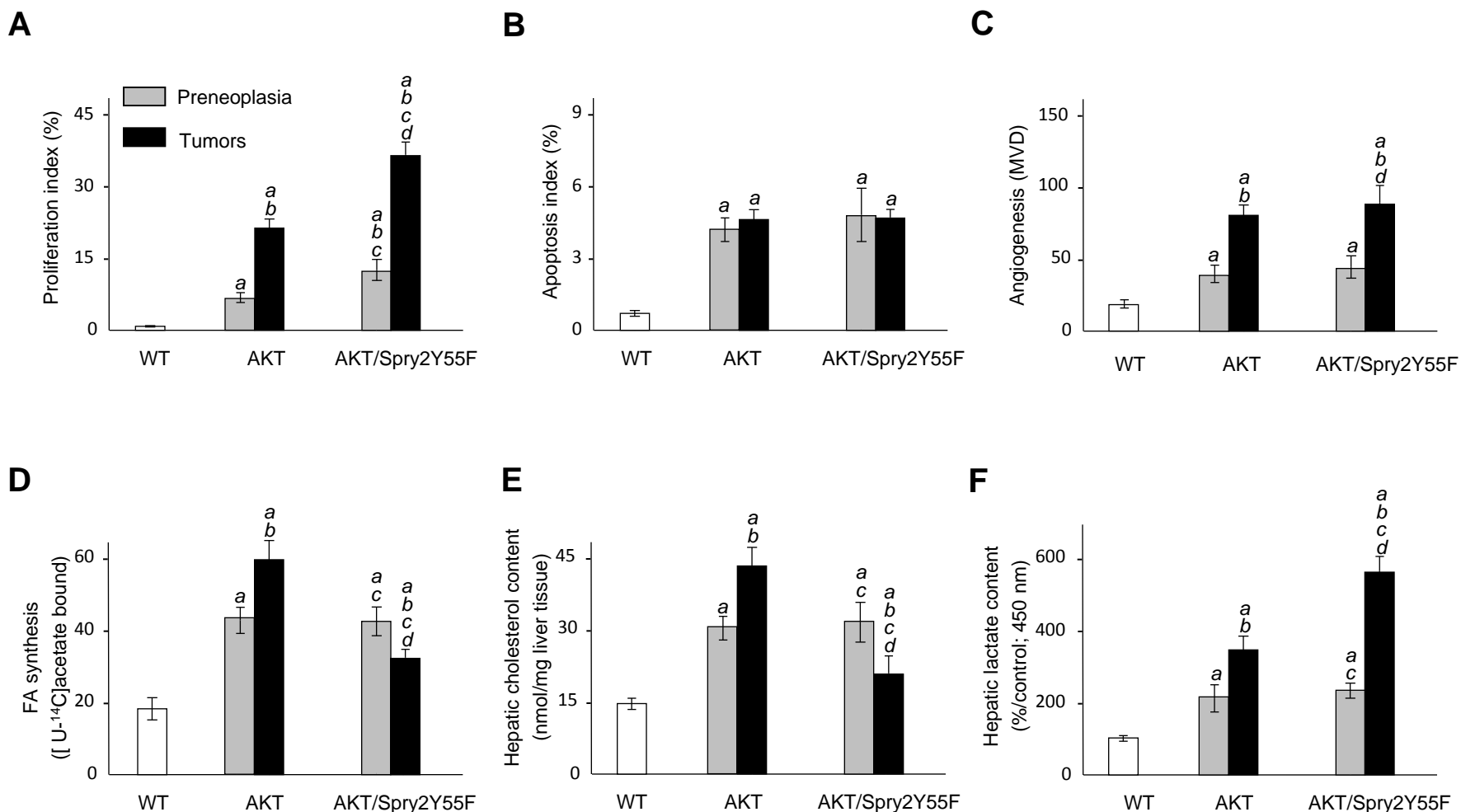
HA-AKT

V5-Spry2Y55F

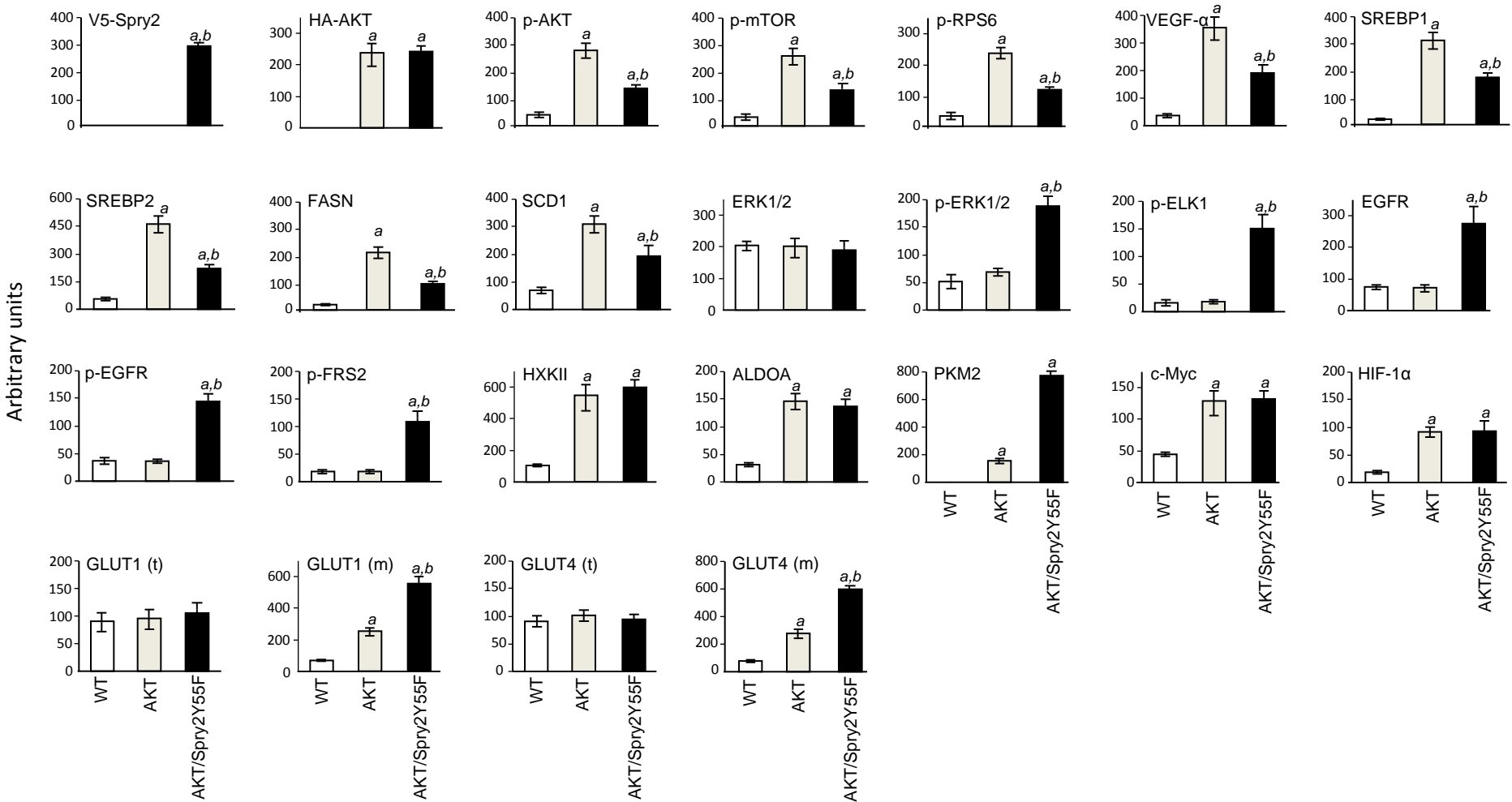
Merged



Supplementary Fig. 2. Co-expression of HA-AKT and V5-Spry2Y55F in AKT/Spry2Y55F liver tumors. Co-localization of HA-AKT (red) and V5-Spry2Y55F (green) in AKT/Spry2Y55F liver tumors as assessed by immunofluorescence. Magnification: 200 x.

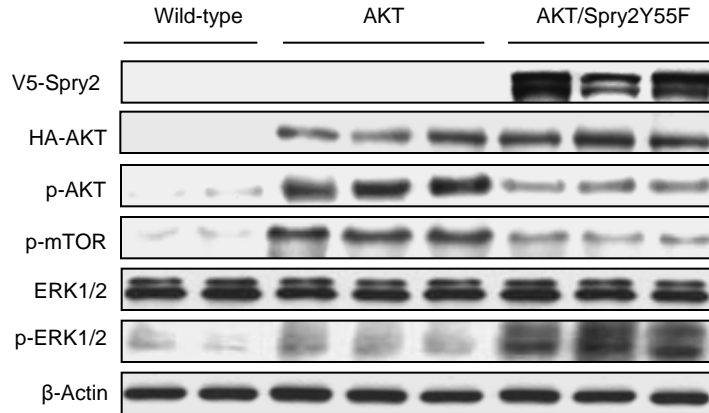


Supplementary Fig. 3. Proliferation and glycolysis are increased in AKT/Spry2Y55F HCCs. (A) Proliferation, (B) apoptosis, (C) angiogenesis (microvessel density, MVD), (D) fatty acid synthesis, (E) hepatic cholesterol content and (F) hepatic lactate content in wild-type (WT) livers, Spry2Y55F livers, preneoplasia and liver tumors developed in AKT and AKT/Spry2Y55F mice. Six to ten samples per group per assay were analyzed. Each bar represents mean \pm SD. Tukey-Kramer test: $P < 0.001$, a, vs. wild-type livers; b, vs. AKT preneoplastic liver; c, v.s. AKT HCCs; d, vs. AKT/Spry2Y55F preneoplastic liver.

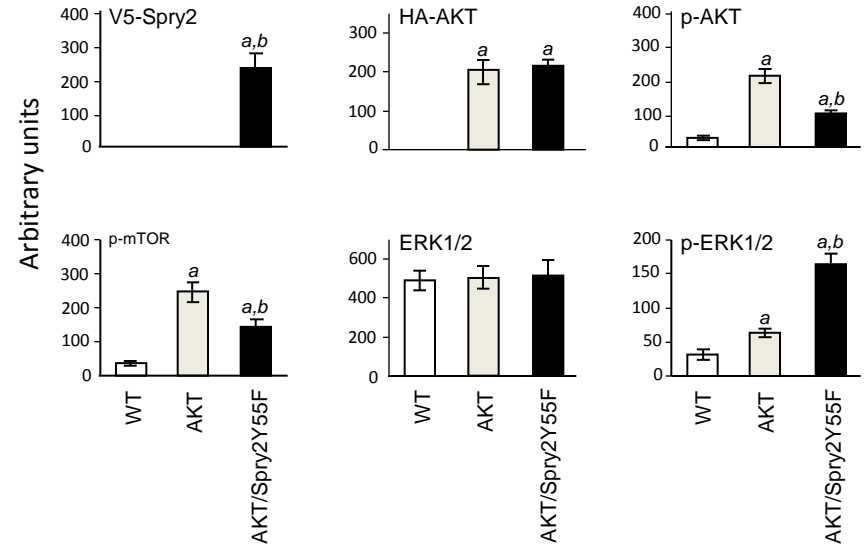


Supplementary Fig. 4. Chemiluminescence analysis of immunoblot analysis for AKT/mTOR, MAPK and glycolysis pathways in wild-type (WT) livers, AKT, and AKT/Spry2Y55F HCCs. For GLUT1 and GLUT4, both total (*t*) and membranous (*m*) levels were determined. Optical densities were normalized to β -Actin values and expressed in arbitrary units. Each bar represents mean \pm SD. Tukey-Kramer test: $P < 0.0001$ *a*, vs. normal liver; *b*, vs. AKT HCCs.

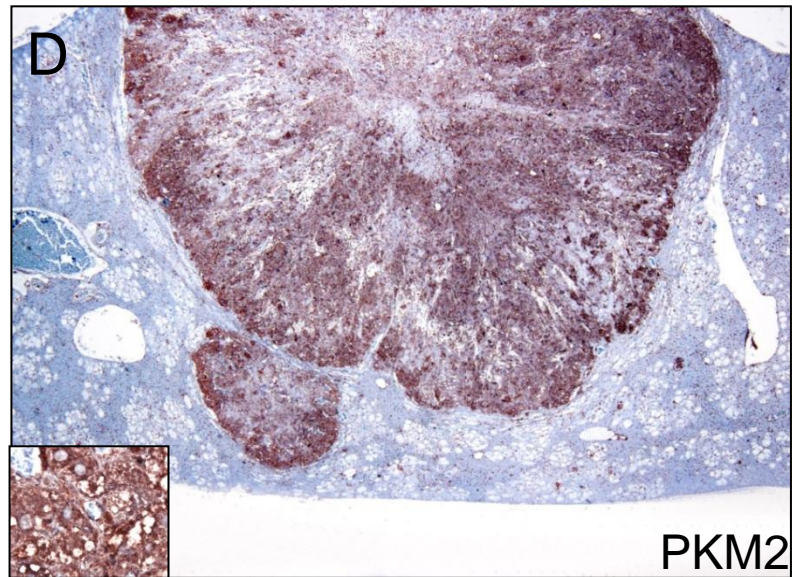
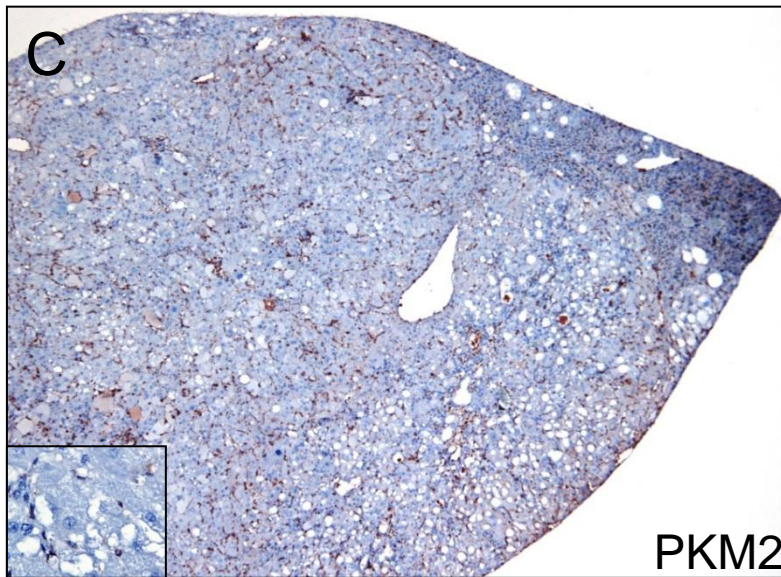
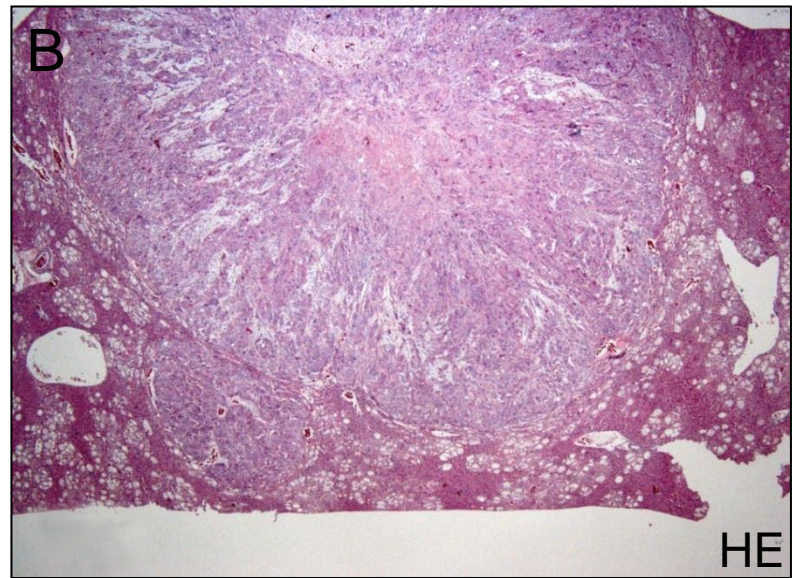
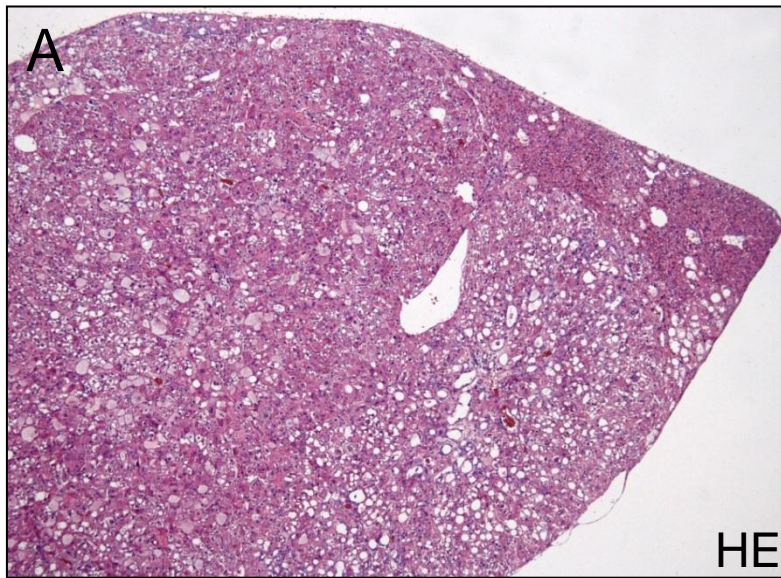
A



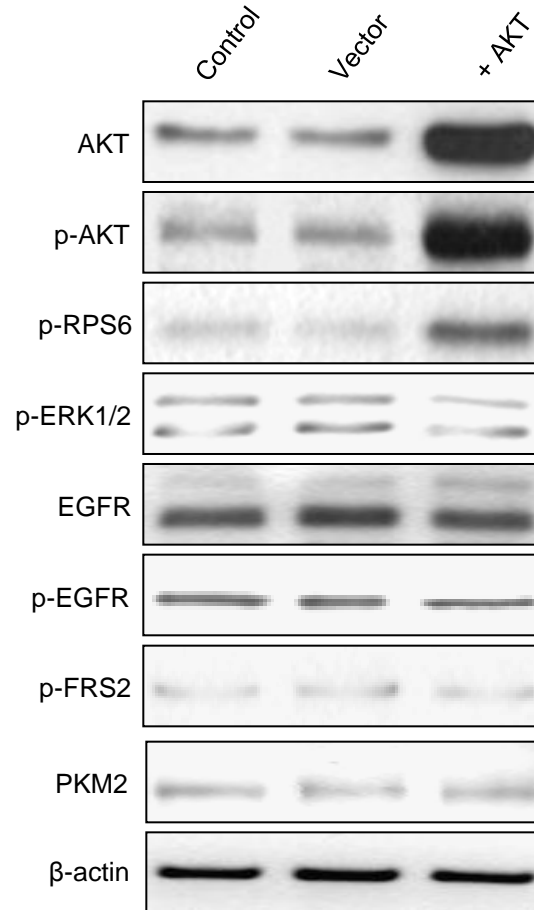
B



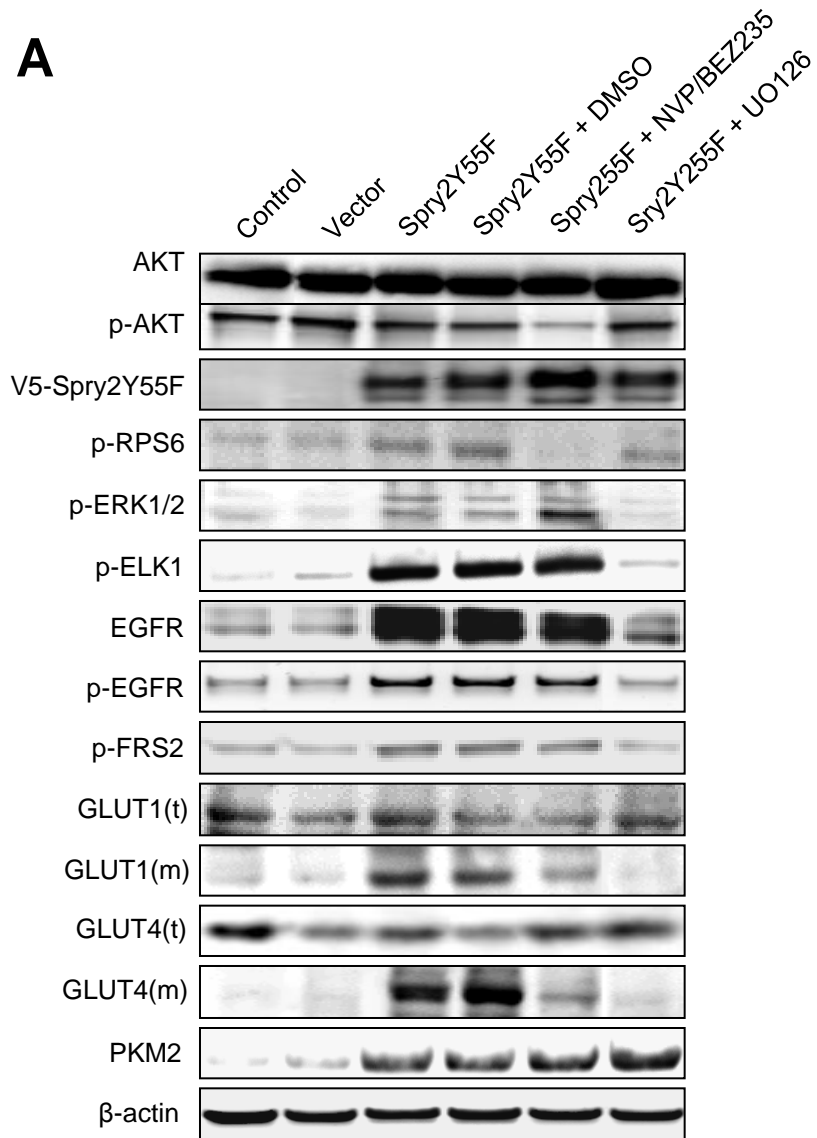
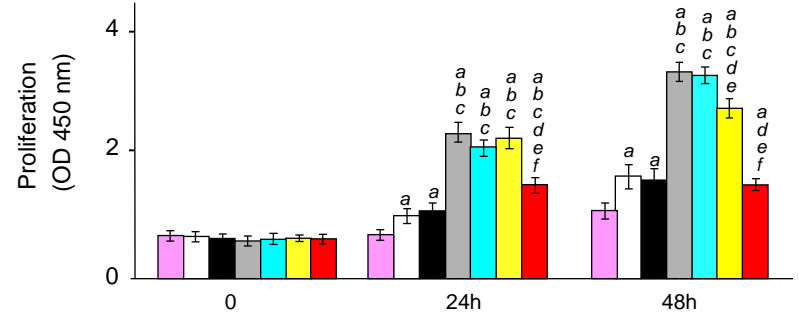
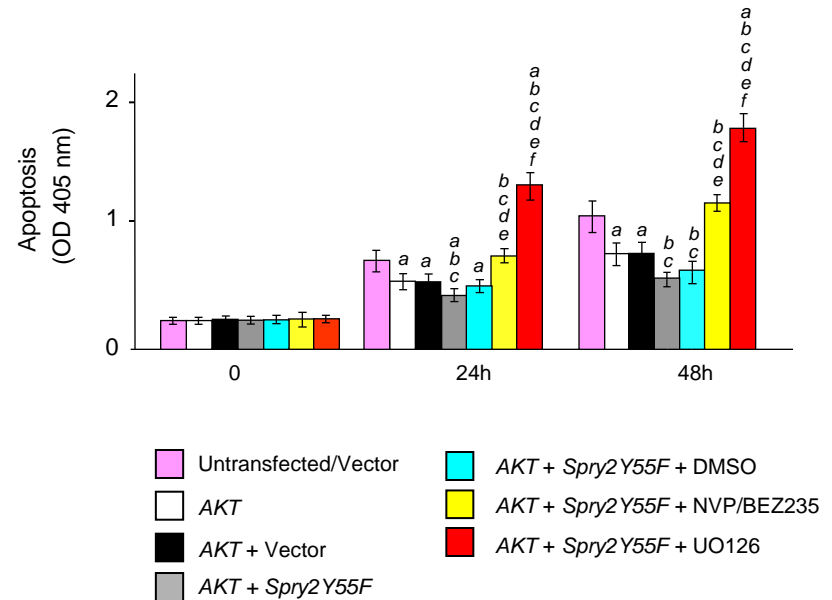
Supplementary Fig. 5 (A) Immunoblotting and (B) Chemiluminescence analysis of the immunoblot analysis for AKT/mTOR and ERK/MAPK signaling pathways in wild-type (WT) livers, AKT, and AKT/Spry2Y55F preneoplastic liver lesions. At least six samples per each group were analyzed. Optical densities were normalized to β -Actin values and expressed in arbitrary units. Each bar represents mean \pm SD. Tukey-Kramer test: $P < 0.0001$ a, vs. normal liver; b, vs. AKT preneoplastic lesions.



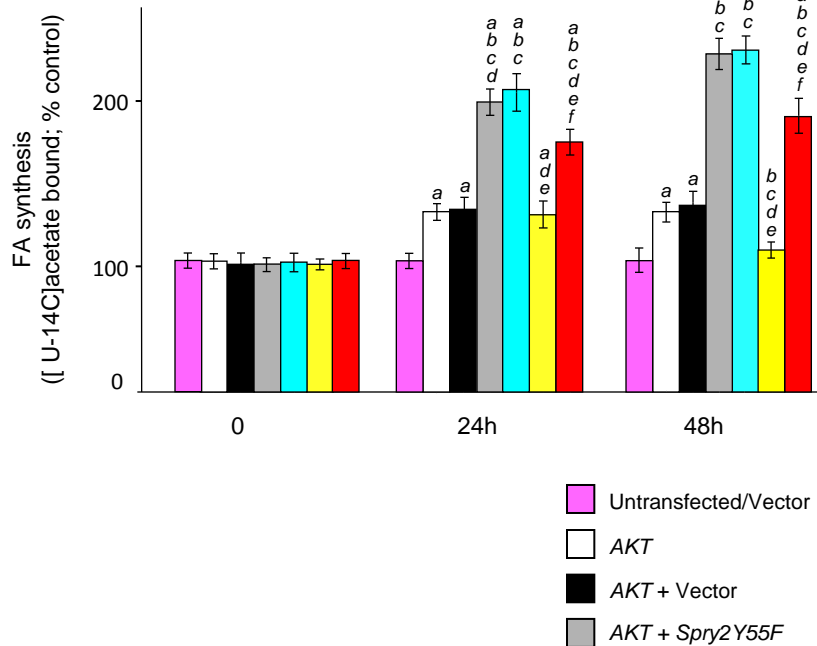
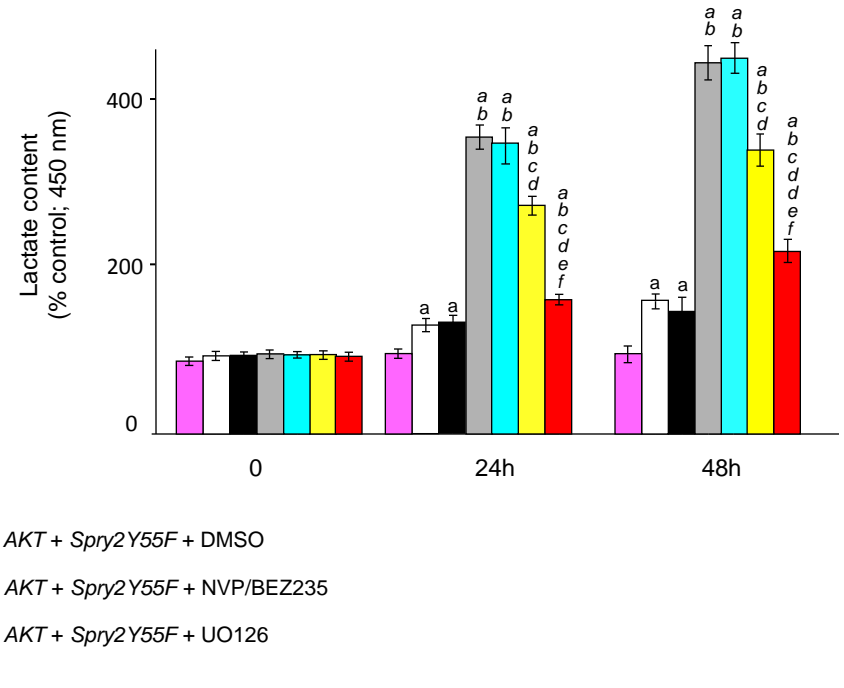
Supplementary Fig. 6. Immunohistochemical staining of PKM2 in AKT (A,C) and AKT/Spry2Y55F (B,D) HCCs. (C) Staining for PKM2 is confined to non-parenchymal cells and absent in malignant hepatocytes in AKT mice. (D) Strong PKM2 immunostaining in neoplastic hepatocytes of an AKT/Spry2 liver HCC. Original Magnification: 40x, except insets (400x).



Supplementary Fig. 7. Overexpression of AKT by stable transfection in the HLE cell line is associated with mTOR activation. Representative immunoblotting showing that successful overexpression of AKT in HLE cells triggers activation of the mTOR cascade (as indicated by phosphorylation of RPS6), but it has no effect on the levels of ERK cascade as well as on activation of EGFR, FRS2, and levels of PKM2.

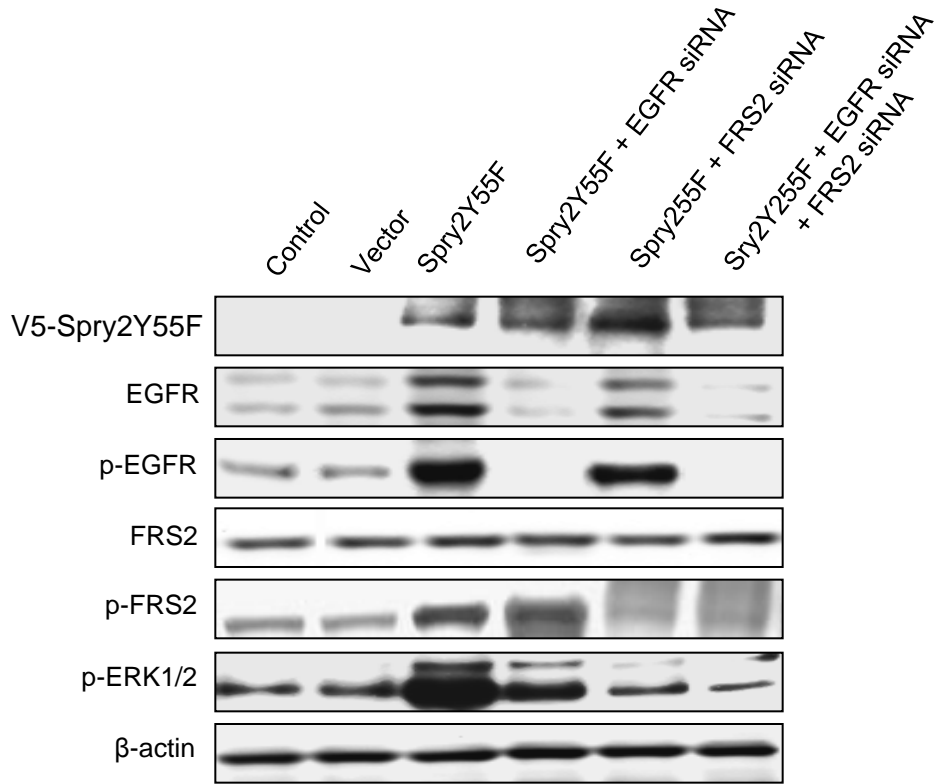
A**B****C**

Supplementary Fig. 8. ERK/MAPK but not AKT/mTOR suppression significantly inhibits cell proliferation induced by *Spry2Y55F* in HLE cells overexpressing *AKT*. (A) Protein levels as analyzed by immunoblotting. (B) Proliferation and (C) apoptosis in HLE cells. Total (*t*) and membranous (*m*) GLUT1 and GLUT4 levels were determined. Data from HLE cells transfected with empty vector were equivalent to those obtained in untransfected cells and were thus merged. Each bar represents mean \pm SD of 3 independent experiments conducted in triplicate. Tukey-Kramer test: $P < 0.0001$ *a*, vs. untransfected cells; *b*, vs. *AKT* transfected cells; *c*, vs. cells transfected with *AKT* and empty vector; *d*, vs. *AKT* and *Spry2Y55F*-transfected cells; *e*, vs. *AKT* and *Spry2Y55F*-transfected cells treated with DMSO; *f*, vs. *AKT* and *Spry2Y55F*-transfected cells treated NVP/BEZ235.

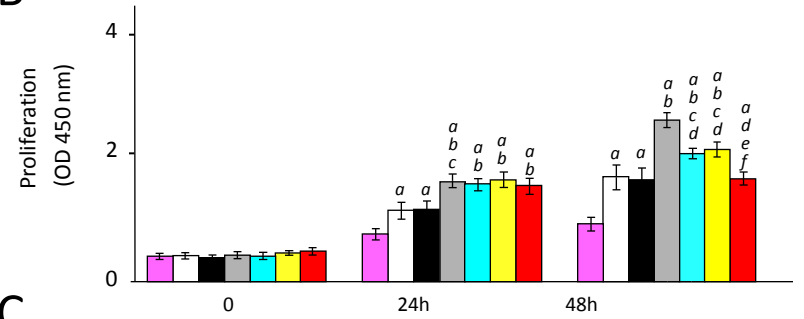
A**B**

Supplementary Fig. 9. Effect of treatment with the PI3K/mTOR dual inhibitor, NVP/BEZ235, or the MAPK inhibitor, UO126, on lipogenesis (A) and glycolysis (B) in the HLE cell line stably transfected with AKT cDNA. Each bar represents mean \pm SD of 3 independent experiments conducted in triplicate. Data from HLE cells transfected with empty vector were equivalent to those obtained in untransfected cells and were thus merged. Tukey-Kramer test: $P < 0.001$ a, vs. untransfected cells; b, vs. AKT transfected cells; c, vs. AKT and empty vector transfected cells; d, vs. AKT and *Spry2Y55F* transfected cells; e, vs. AKT and *Spry2Y55F* transfected cells treated with DMSO (solvent); f, vs. AKT and *Spry2Y55F* transfected cells treated NVP/BEZ235.

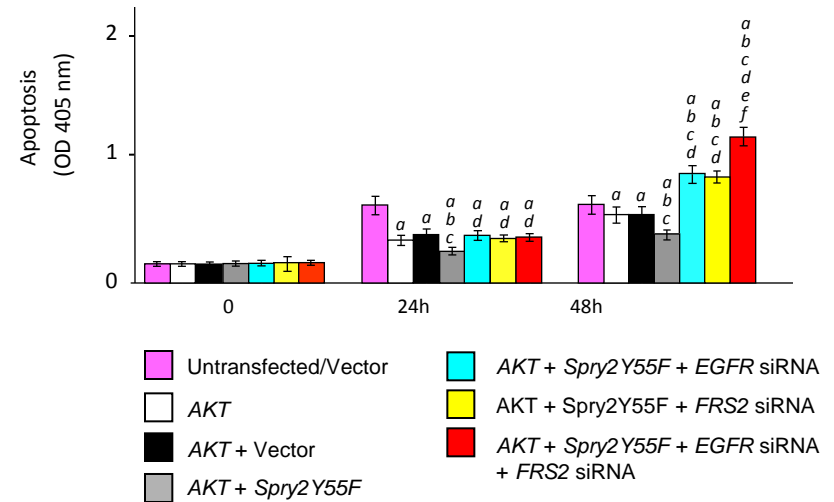
A



B

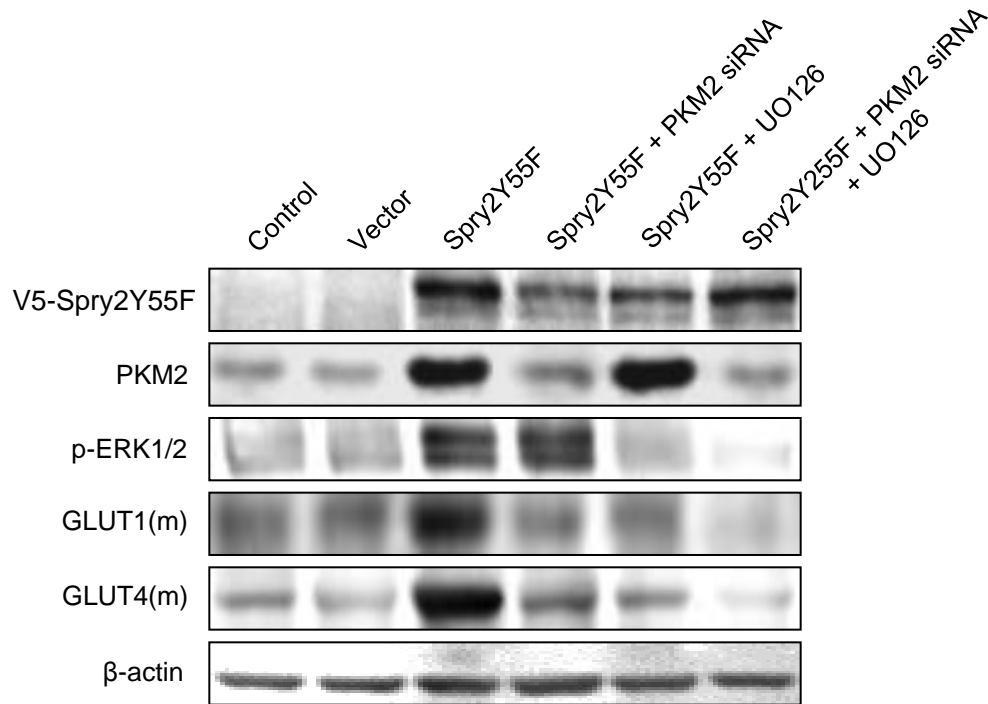


C

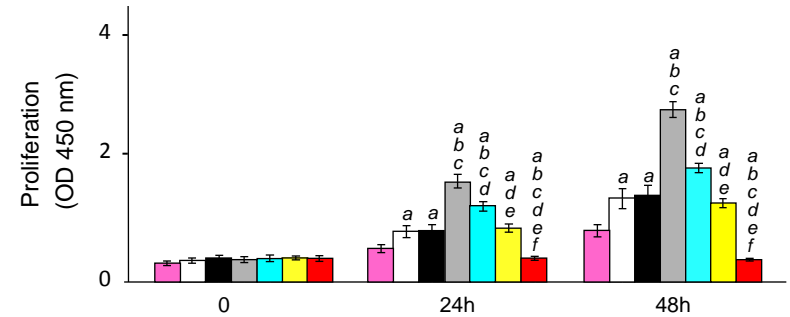


Supplementary Fig. 10. Suppression of EGFR and/or FRS2 significantly inhibits cell proliferation induced by *Spry2Y55F* in HLE cells overexpressing AKT. (A) Protein levels as analyzed by immunoblotting. (B) Proliferation and (C) apoptosis in HLE cells. Each bar represents mean \pm SD of 3 independent experiments conducted in triplicate. Data from HLE cells transfected with empty vector were equivalent to those obtained in untransfected cells and were thus merged. Tukey-Kramer test: $P < 0.0001$ a, vs. untransfected HLE cells; b, vs. AKT transfected cells; c, vs. cells transfected with AKT and empty vector; d, vs. AKT and *Spry2Y55F* transfected cells; d, vs. AKT and *Spry2Y55F* transfected cells in which EGFR was silenced by siRNA; e, vs. AKT and *Spry2Y55F* transfected cells in which FRS2 was silenced by siRNA; f, vs. AKT and *Spry2Y55F* transfected cells in which EGFR and FRS2 were concomitantly silenced by siRNA.

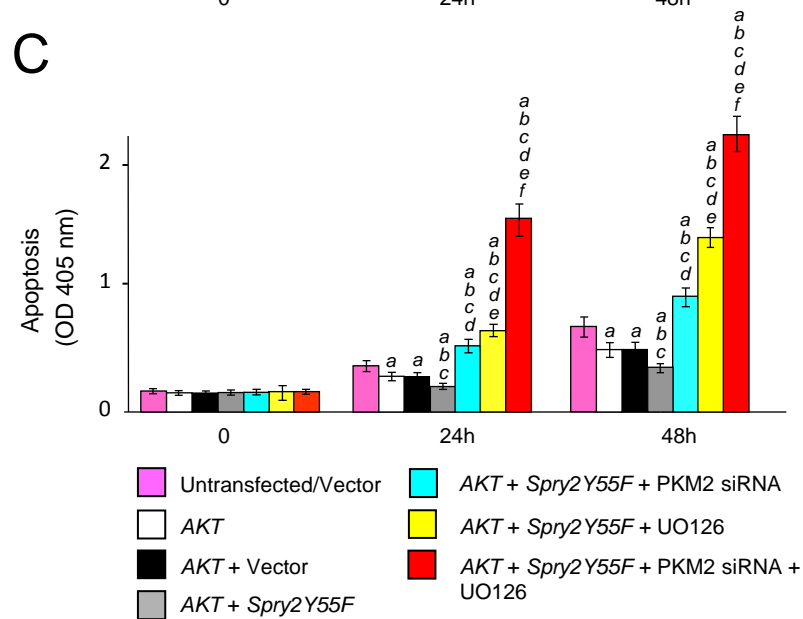
A



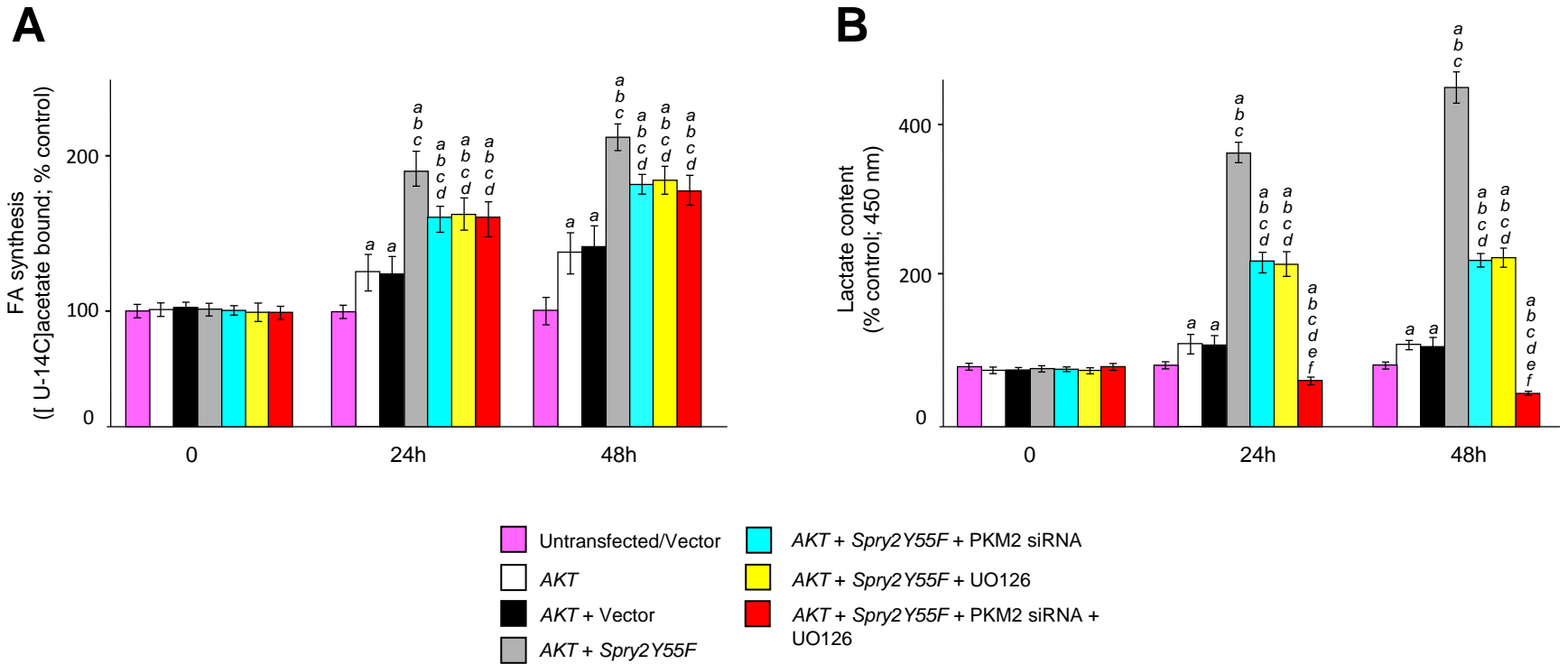
B



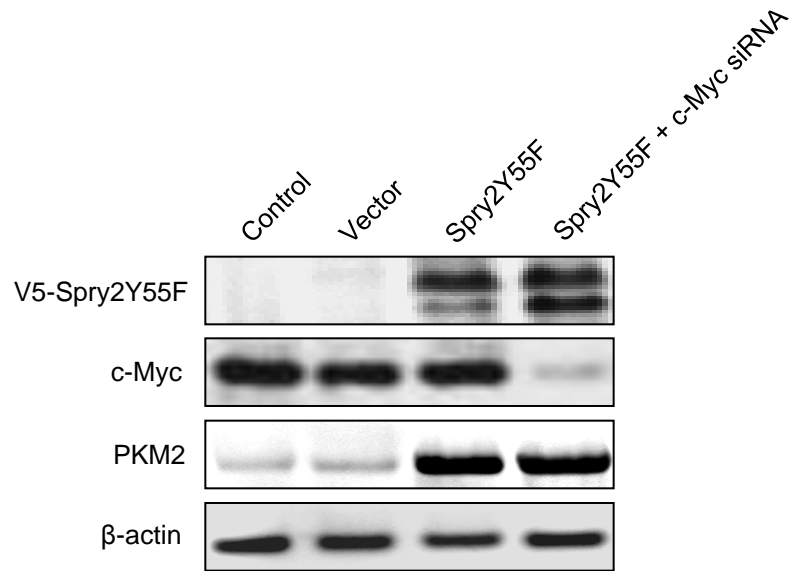
C



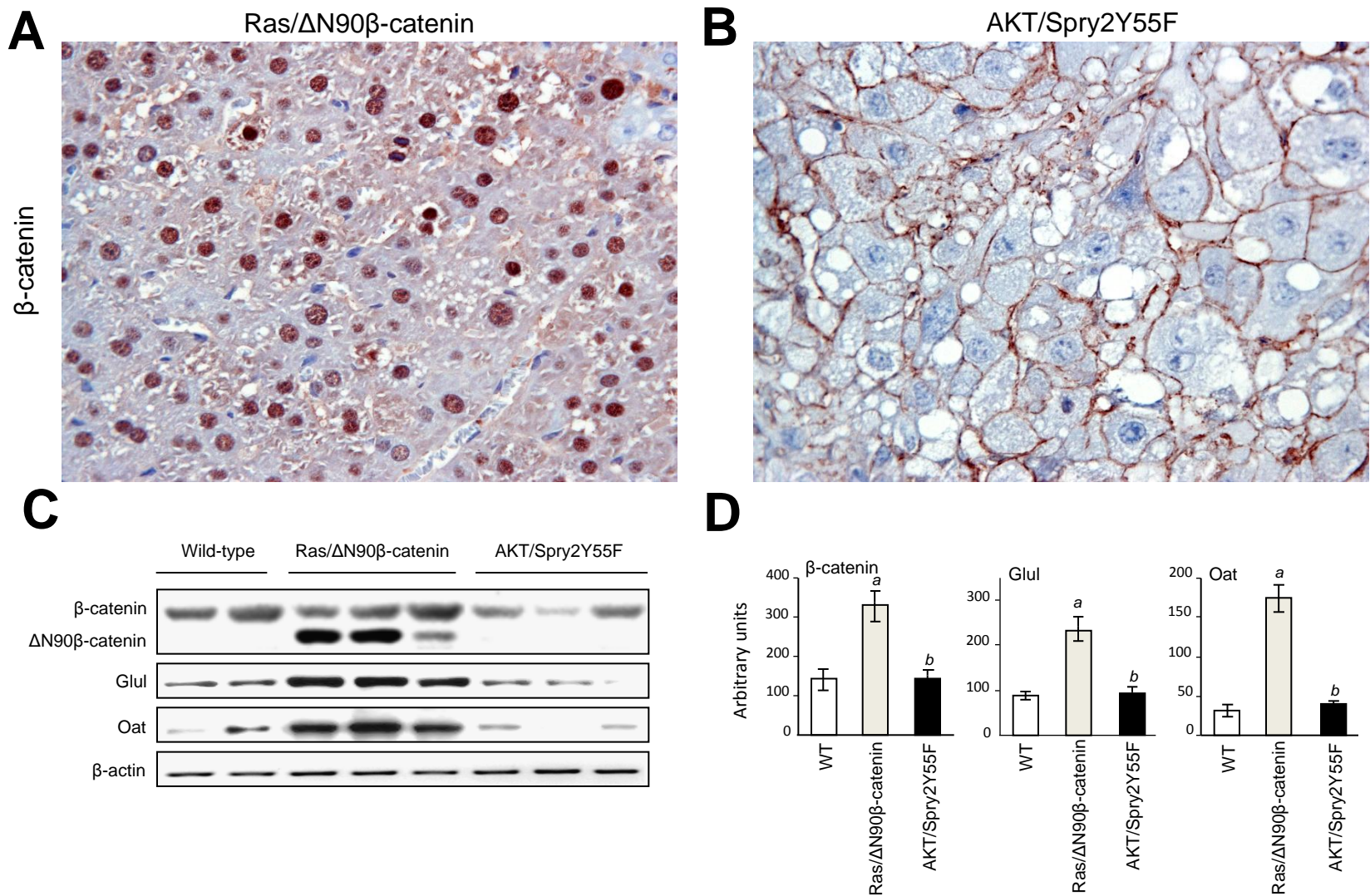
Supplementary Fig. 11. Combined inhibition of ERK/MAPK and PKM2 cascades completely abolishes the growth properties of HLE cells overexpressing AKT and Spry2Y55F. (A) Protein levels as analyzed by immunoblotting. (B) Proliferation and (C) apoptosis. Total (*t*) and membranous (*m*) GLUT1 and GLUT4 levels were determined. Data from HLE cells transfected with empty vector were equivalent to those obtained in untransfected cells and were thus merged. Each bar represents mean \pm SD of 3 independent experiments conducted in triplicate. Tukey-Kramer test: $P < 0.0001$ *a*, vs. untransfected cells; *b*, vs. AKT transfected cells; *c*, vs. cells transfected with AKT and empty vector; *d*, vs. AKT and Spry2Y55F transfected cells; *e*, vs. AKT and Spry2Y55F transfected cells treated with PKM2 siRNA; *f*, vs. AKT and Spry2Y55F transfected cells treated with UO126.



Supplementary Fig. 12. Effect of treatment with the MAPK inhibitor, UO126, either alone or in combination with silencing of PKM2 via siRNA, on lipogenesis (A) and glycolysis (B) in the HLE cell line stably transfected with AKT cDNA. Each bar represents mean \pm SD of 3 independent experiments conducted in triplicate. Data from HLE cells transfected with empty vector were equivalent to those obtained in untransfected cells and were thus merged. Tukey-Kramer test: $P < 0.001$ a, vs. untransfected cells; b, vs. AKT transfected cells; c, vs. cells transfected with AKT and empty vector; d, vs. AKT and *Spry2Y55F* transfected cells; e, vs. AKT and *Spry2Y55F* transfected cells treated with PKM2 siRNA; f, vs. AKT and *Spry2Y55F* transfected cells treated with UO126.



Supplementary Fig. 13. Activation of PKM2 is c-Myc independent in HLE cells overexpressing *AKT* and *Spry2Y55F*. HLE cells, stably transfected with *AKT*, were subjected to c-Myc silencing via siRNA. Protein levels were analyzed by immunoblotting 48 hours after c-Myc siRNA transfection.



Supplementary Fig. 14. Lack of activation of the WNT/ β -catenin pathway in AKT/Spry2 tumors. (A) Strong nuclear accumulation of β -catenin in a mouse model overexpressing an activated form of β -catenin and N-Ras that was used as a positive control [18]. (B) β -catenin staining is limited to the membranous compartment of AKT/Spry2Y55F HCCs. Representative immunoblotting (C) and chemiluminescence analysis (D) of β -catenin and its targets (Glul, glutamine synthetase, and Oat, ornithine aminotransferase) in wild-type (WT) livers, Ras/ Δ N90 β -catenin and AKT/Spry2Y55F HCCs. At least six samples per group were analyzed. Optical densities were normalized to β -Actin values and expressed in arbitrary units. Each *bar* represents mean \pm SD. Tukey-Kramer test: $P < 0.0001$ *a*, vs. normal liver; *b*, vs. Ras/ Δ N90 β -catenin HCC.